Chemical Bonding in Hypervalent Molecules Revised. 2.† Application of the Atoms in Molecules Theory to Y_2XZ and Y_2XZ_2 (Y = H, F, CH_3; X = O, S, Se; Z = O, S) Compounds

J. A. Dobado,‡ Henar Martínez-García,‡ José Molina Molina,*,‡ and Markku R. Sundberg*,§

Contribution from the Grupo de Modelización y Diseño Molecular, Instituto de Biotecnología, Campus Fuentenueva, Universidad de Granada, E-18071 Granada, Spain, and Laboratory of Inorganic Chemistry, Department of Chemistry, P.O. Box 55 (A.I. Virtasen aukio 1), FIN-00014, University of Helsinki, Helsinki, Finland

Received August 7, 1998. Revised Manuscript Received November 6, 1998

Abstract: The atoms in molecules theory has been applied to analyze bonding properties in potentially hypervalent structures with chalcogen (O, S, or Se)−chalcogen (O or S) bonds. The topological analyses [based upon the electron charge density $\rho(r)$, its Laplacian $\nabla^2\rho(r)$, bond ellipticity, and local energy density $E_d(r)$] and the charges clearly displayed the dependence of the bonding properties with the central atom: (a) When the central atom is oxygen, the main electron charge concentration remains in the surroundings of the central atom, yielding a very weak coordinate bond. (b) Bonding to the central sulfur and selenium atoms is consistent with a model of a highly polarized σ-bond, its strength depending mainly on electrostatic interactions, so no evidence was found for double bonding, which has so far been the conventional way to describe the interaction in these systems. The equilibrium geometries were optimized by both density functional theory with a hybrid functional (B3LYP) and ab initio methods at the MP2(full) level, using the 6-311+G* basis set.

I. Introduction

The bonding nature in hypervalent molecules has been controversial for years, including pnicogen or chalcogen (groups 15 and 16 in IUPAC nomenclature, respectively) compounds.[2−18] The description of the structure and bonding in these hypervalent compounds was connected with the possible involvement of virtual d orbitals in the bonding. For the first-row atoms, the d basis functions in the ab initio calculations play a role as polarization functions augmenting the quality of the sp basis set. However, for transition metals this function provides a description for the valence d orbitals. For the second-row elements, there appears to be no clear demarcation with use of d functions between *normal octet* and *hypervalent* species.

The majority of accurate ab initio calculations[2,3,7,16,18−38] now agree that the d function acts mostly as a polarization function for second-row atoms, compensating for the inflexibility of the sp basis set. The above-mentioned studies are devoted mainly to pnicogen oxides and sulfides, including a very recent contribution by our group.[1]

One key point to be addressed is the interpretation and definition of the hypervalent-molecule concept, as a compound

* Correspondence may be addressed to the authors *via* E-mail: jmolina@goliat.ugr.es, sundberg@cc.helsinki,fi.

† For part 1 see ref 1.

‡ Universidad de Granada.

§ University of Helsinki.

(1) Dobado, J. A.; Martínez-García, H.; Molina, J.; Sundberg, M. R. *J. Am. Chem. Soc.* **1998**, *120*, 8461.
(2) Wallmeier, H.; Kutzelnigg, W. *J. Am. Chem. Soc.* **1979**, *101*, 2804.
(3) Kutzelnigg, W. *Angew. Chem., Int. Ed. Engl.* **1984**, *23*, 272.
(4) Kutzelnigg, W. *Pure Appl. Chem.* **1977**, *49*, 981.
(5) Bollinger, J. C.; Houriet, R.; Kern, C. W.; Perret, D.; Weber, J.; Yvernault, T. *J. Am. Chem. Soc.* **1985**, *107*, 5352.
(6) Keil, F.; Kutzelnigg, W. *J. Am. Chem. Soc.* **1975**, *97*, 3623.
(7) Messmer, R. P. *J. Am. Chem. Soc.* **1991**, *113*, 433.
(8) Schmidt, M. W.; Gordon, M. S. *J. Am. Chem. Soc.* **1985**, *107*, 1922.
(9) Boatz, J. A.; Gordon, M. S. *J. Comput. Chem.* **1986**, *7*, 306.
(10) Streitwieser, A.; McDowell, R. S.; Glaser, R. *J. Comput. Chem.* **1987**, *8*, 788.
(11) Streitwieser, A.; Rajca, A.; McDowell, R. S.; Glaser, R. *J. Am. Chem. Soc.* **1987**, *109*, 4184.
(12) Schneider, W.; Thiel, W.; Komornicki, A. *J. Phys. Chem.* **1988**, *92*, 5611.
(13) Maglagan, G. A. R. *J. Phys. Chem.* **1990**, *94*, 3373.
(14) Gilheany, D. G. *The Chemistry of Organophosphorous Compounds*; Wiley-Interscience: Chichester, 1992.
(15) Gilheany, D. G. *Chem. Rev.* **1994**, *94*, 1339.
(16) Kutzelnigg, W. *J. Mol. Struct. THEOCHEM* **1988**, *169*, 403.
(17) Sandblom, N.; Ziegler, T.; Chivers, T. *Can. J. Chem.* **1996**, *74*, 2363.
(18) Reed, A. E.; Schleyer, P. v. R. *J. Am. Chem. Soc.* **1990**, *112*, 1434.
(19) Ehrhardt, C.; Ahlrichs, R. *Theor. Chim. Acta* **1985**, *68*, 231.
(20) Heinzmann, R.; Ahlrichs, R. *Theor. Chim. Acta* **1976**, *42*, 33.
(21) Cruickshank, D. W. J.; Eisenstein, M. *J. Mol. Struct.* **1985**, *130*, 143.
(22) Cruickshank, D. W. J. *J. Mol. Struct.* **1985**, *130*, 177.
(23) Cruickshank, D. W. J.; Eisenstein, M. *J. Comput. Chem.* **1987**, *8*, 6.
(24) Reed, A. E.; Weinhold, F. *J. Am. Chem. Soc.* **1986**, *108*, 3586.
(25) Reed, A. E.; Schleyer, P. v. R. *Chem. Phys. Lett.* **1987**, *133*, 553.
(26) Foster, J. P.; Weinhold, F. *J. Am. Chem. Soc.* **1980**, *102*, 7211.
(27) Reed, A. E.; Weinstock, R. B.;Weinhold, F. *J. Chem. Phys.* **1985**, *83*, 735.
(28) Reed, A. E.; Weinhold, F. *J. Chem. Phys.* **1985**, *83*, 1736.
(29) Cooper, D. L.; Cunningham, T. P.; Gerratt, J.; Karadakov, P. B.; Raimondi, M. *J. Am. Chem. Soc.* **1994**, *116*, 4414.
(30) Gerratt, J.; Lipscomb, W. N. *Proc. Natl. Acad. Sci. U.S.A.* **1968**, *59*, 332.
(31) Cooper, D. L.; Garratt, J.; Raimondi, M. *Adv. Chem. Phys.* **1987**, *69*, 319.
(32) Cooper, D. L.; Gerratt, J.; Raimondi, M. *Chem. Rev.* **1991**, *91*, 929.
(33) Ladner, R. C.; Goddard, W. A. *J. Chem. Phys.* **1969**, *51*, 1073.
(34) Magnusson, E. *J. Am. Chem. Soc.* **1990**, *112*, 7940.
(35) Magnusson, E. *J. Am. Chem. Soc.* **1993**, *115*, 1051.
(36) Harcourt, R. D. *J. Mol. Struct.* **1992**, *259*, 155.
(37) Harcourt, R. D. *J. Mol. Struct.* **1993**, *300*, 243.
(38) Legon, A. C.; Millen, D. J. *J. Chem. Soc. A* **1968**, 1736.

10.1021/ja9828206 CCC: $18.00
Published on Web 03/19/1999

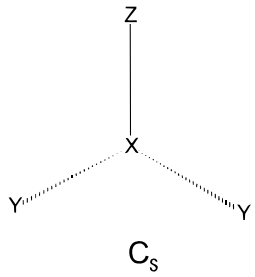

C_s

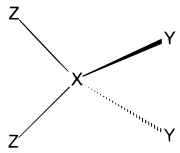

C_{2V}

	X	Y	Z
1	O	H	O
2	O	F	O
3	O	Me	O
4	O	H	S
5	O	F	S
6	O	Me	S
7	S	H	O
8	S	F	O
9	S	Me	O
10	S	H	S
11	S	F	S
12	S	Me	S
13	Se	H	O
14	Se	F	O
15	Se	Me	O
16	Se	H	S
17	Se	F	S
18	Se	Me	S

	X	Y	Z
19	O	H	--
20	O	F	--
21	O	Me	--
22	S	H	--
23	S	F	--
24	S	Me	--
25	Se	H	--
26	Se	F	--
27	Se	Me	--
28	O	H	O
29	O	F	O
30	O	Me	O
31	O	H	S
32	O	F	S
33	O	Me	S
34	S	H	O
35	S	F	O
36	S	Me	O
37	S	H	S
38	S	F	S
39	S	Me	S
40	Se	H	O
41	Se	F	O
42	Se	Me	O
43	Se	H	S
44	Se	F	S
45	Se	Me	S

Figure 1. Structures of compounds **1**−**45**.

that violates the octet rule. Cioslowski *et al.*[39] provided a precise definition of the hypervalent molecule, and pointed out the necessity of analyzing the computed wavefunction in a rigorous manner.

"*This means, that the interpretative tools utilized in such an analysis have to employ definitions that are fully independent of the methods used in calculations of the wave functions and the character of the analyzed molecules.*"[39]

The systems studied in this paper are compounds with chalcogen (O, S, Se)−chalcogen (O, S) bonds (Figure 1). Compounds of great interest in chemistry, such as sulfoxide and sulfones, are included, together with the sulfur analogs thiosulfoxides and thiosulfones. Oxygen and selenium analogs have also been taken into consideration, in order to study the bond nature in the compounds having chalogen−chalcogen bonds. Structures **19**−**27** following the octet rule have been included for comparison. Theoretical calculations for several of the above mentioned compounds are described in the literature, and the most accurate results are summarized in Table 1. To our knowledge, no previous theoretical calculations have been performed for structures **4**, **5**, **16**−**18**, **28**−**33**, and **37**−**45**.

Several compounds depicted in Figure 1 present OF or SF bonds; difficulties in the theoretical description[40,41] for these bonds have arisen, especially with Møller−Plesset theory. This problem is resolved by using CCSD(T) calculations;[40,42] the use of B3LYP has also been proposed as an economical alternative in the description of the OF and SF bonds.[40,43,44]

Recently, calculations have been reported for the equilibrium

$$Z-X-Y-Z \leftrightarrow Z_2XY$$

Thus, the stability of oxywater compared with that of hydrogen peroxide and its difluoro and dimethyl derivatives has been reported,[45−47] as well as the stability of thiosulfoxides compared with the corresponding disulfides.[48−50] The bonding of S−O in sulfoxide and sulfones is generally accepted as being a double bond with ionic character.

In this context, Reed and Schleyer's work[18] could be considered as a milestone. The results of this paper clearly show that d-back-bonding does not participate, and from a natural localized molecular orbital analysis the S−O bond can be regarded as a partially ionic σ-bond and partial π-bonding through strong n $\rightarrow$ σ^* negative hyperconjugation. Moreover, the GVB calculations of Cunningham *et al.*[51] for SOF_2 and SO_2F_2 show that the S−O bond has essentially a double bond character with the S−O π-bond more polar than the corresponding σ-bond. Accordingly, they found no evidence to support notions of $p_\pi-d_\pi$ back-donation from oxygen to sulfur.

The quantum-mechanical theory of *atoms in molecules* (AIM), proposed by Bader,[52] makes it possible to define atomic and bond properties without resorting to the unjustified identification of basis functions as atomic orbitals.

This theory has been widely used to a great extent in the molecular description of compounds,[52−55] as well as for other hypervalent compounds like phosphonic acid derivatives.[56,57]

(39) Cioslowski, J.; Mixon, S. T. *Inorg. Chem.* **1993**, *32*, 3209.
(40) Lee, T. J.; Rice, J. E.; Dateo, C. E. *Mol. Phys.* **1994**, *228*, 583.
(41) Lee, T. J.; Rice, J. E.; Scuseria, G. E.; Schaefer, G. E. *Theor. Chim. Acta* **1989**, *75*, 81.
(42) Lee, T. J.; Scuseria, G. E. *Quantum Mechanical Electronic Structure Calculations with Chemical Accuracy*; Langhoff, S. R., Ed.; Kluwer: Dordrecht, 1995; pp 47−108.
(43) Lee, T. J.; Bauschlicher, C. W.; Dateo, C. E.; Rice, J. E. *Chem. Phys. Lett.* **1994**, *228*, 583.
(44) Torrent, M.; Duran, M.; Sola, M. *J. Mol. Struct. THEOCHEM* **1996**, *362*, 163.
(45) Huang, H. H.; Xie, Y. M.; Schaefer, H. F. *J. Phys. Chem.* **1996**, *100*, 6076.
(46) Jursic, B. S. *J. Mol. Struct. THEOCHEM* **1996**, *366*, 97.
(47) Schalley, C. A.; Harvey, J. N.; Schröder, D.; Schwarz, H. *J. Phys. Chem. A* **1998**, *102*, 1021.
(48) Sola, M.; Mestres, J.; Carbo, R.; Duran, M. *J. Am. Chem. Soc.* **1994**, *116*, 5909.
(49) Bickelhaupt, F. M.; Sola, M.; Schleyer, P. v. R. *J. Comput. Chem.* **1995**, *16*, 465.
(50) Steudel, R.; Drozdova, Y.; Miaskiewicz, K.; Hertwig, R. H.; Koch, W. *J. Am. Chem. Soc.* **1997**, *119*, 1990.
(51) Cunningham, T. P.; Cooper, D. L.; Gerratt, J.; Karadakov, P. B.; Raimondi, M. *J. Chem. Soc. Faraday Trans.* **1997**, *93*, 2247.
(52) Bader, R. F. W. *Atoms in Molecules: a quantum theory*; Clarendon Press: Oxford, 1990.
(53) Fan, M. F.; Jia, G. C.; Lin, Z. Y. *J. Am. Chem. Soc.* **1996**, *118*, 9915.
(54) Platts, J. A.; Howard, S. T.; Bracke, B. R. F. *J. Am. Chem. Soc.* **1996**, *118*, 2726.
(55) Heinemann, C.; Muller, T.; Apeloig, Y.; Schwarz, H. *J. Am. Chem. Soc.* **1996**, *118*, 2023.
(56) Hernández-Laguna, A.; Saínz-Díaz, C. I.; Smeyers, Y. G.; de Paz, J. L. G.; Ruano, E. G. *J. Phys. Chem.* **1994**, *98*, 1109.
(57) Saínz-Díaz, C. I.; Hernández-Laguna, A.; Smeyers, Y. G. *J. Mol. Struct. THEOCHEM* **1997**, *390*, 127.

Table 1. Previously Reported Theoretical Calculations

	methods	Z−X	X−Y	∠Z−X−Y	∠Y−X−Y	∠Z−X−Z	ref
1	CCSD(T)/DZP	1.578	0.974		105.8		45
	CCSD(T)/TZ2P+f	1.549	0.967		106.4		45
2	B3LYP/6-311++G(2d)	1.165	1.651	110.3			46
3	B3LYP/6-311++G(d,p)	1.489	1.448	108.0	114.1		47
6	QCISD/6-31G*	1.511	1.382	109.8	87.3		44
7	MP2/6-311G**	1.493	1.373	110.2	85.7		63
8	MP2/[a]	1.445	1.626	107.1	92.0		80
	MP2/6-31G*	1.409	1.571	106.7	92.4		81
9	HF/6-311++G**	1.490	1.797	106.4	98.3		82
10	MP2/6-311++G(2df,2p)	1.979	1.355	108.3	89.6		49
11	MP2/6-311G(2d,2p)	1.877	1.636	108.2	91.3		49
12	MP2/6-311G(2d,2p)	1.999	1.809	105.9	96.9		49
13	HF/[a]	1.626	1.476	105.5	90.1		80
	MP2/[a]	1.648	1.499	106.5	86.6		80
14	MP2/[a]	1.587	1.754	105.2	91.3		80
15	HF/[b]	1.638	1.939	103.4	96.0		80
34	HF/[c]	1.444	1.346	108.3	97.7		83
35	HF/3-21G*	1.395	1.511		95.2	124.4	84
36	MP2(full)/6-31+G*	1.472	1.783		103.8	120.9	85

[a] With the (20s15p9d/13s10p3d) Se, (13s8p2d/7s4p2d) O,P, (8s2p/5s2p) H basis. [b] With the 3-21G* Se, 6-31G** C,O basis. [c] With the (7s3p1d/5s3p1d) O, (10s6p1d/7s4p1d) S, (3s/3s) H basis.

In our group the AIM theory has also been used to analyze intermolecular interactions[58,59] and transition metal complexes.[60−62]

Usually, the theoretical bond nature analyses on hypervalent molecules have been performed by different approaches from the obtained electronic wave functions (NBO, GVB, MO analysis, etc.), sometimes ending in contradictory results.[15] Thus, in the interpretation and analysis of the electronic wave function, only observable-based theoretical tools should be applied.[63] Such a rigorous approach yields a concise set of tools that are universally applied to all electronic wave functions. Currently, there is only one general approach available that provides a comprehensive set of observable-based interpretative tools (the topological AIM theory). In this context, theoretical bond nature in hypervalent sulfur molecules has been studied by Cioslowski *et al*.[39,63] These studies show a high ionic nature in the S−O bond. Each of the formally double S−O bonds consists of one highly polarized covalent σ-bond and one almost fully ionic π-bond.

Our group is involved in the study of bond nature in hypervalent molecules and we have already reported the applications of the AIM to the study of bonding in pnicogen (N, P, As)−chalcogen (O, S) bonds.[1] From that study we concluded that the above mentioned bonds may be described as *polar single σ-bonds mainly characterized by electrostatic interactions*. In addition, we have recently tested these results by changing the level and basis sets together with the geometry.[64]

The aim of the present paper is to extend our previous work[1] to chalcogen−chalcogen hypervalent model molecules, focusing on the bonding nature in the framework of the AIM theory.

II. Methods of Calculation

A. General Methods. The DFT (using the hybrid Becke 3-Lee-Yang-Parr (B3LYP) exchange-correlation functional[65,66]) and the MP2(full)[67] calculations have been carried out with the Gaussian 94 package of programs,[68] using the 6-311+G* basis set. The structures presented were fully optimized at the mentioned levels of theory, with constrained C_s symmetry for **1**−**18** and C_{2v} for **19**−**45**. Vibrational analyses were used to check the nature of the stationary points, and none of the structures **1**−**45** presented imaginary frequencies (true minima) at either B3LYP and MP2 levels with the 6-311+G* basis. For structures **2**, **5**, **29**, and **32**, with O−F or S−F bonds, difficulties have been found at the MP2 theoretical level. Accordingly, additional calculations at the CCD level were carried out for these structures. For structure **29** no stationary points were found in the CCD and MP4(full) potential energy surfaces. The Bader analyses have been performed with the AIMPAC series of programs[69] by using the DFT and MP2 wave functions as input, as described in AIM theory.[52,70] The $\nabla^2\rho(r)$ contour map representations of the different structures were obtained by using the MORPHY program.[71] The atomic charges have been calculated with use of the AIMPAC series of programs,[69] by integration over the basin of every atom in the Bader framework.

B. Overview of the Atoms in Molecules Theory. The topology of the electronic charge density ($\rho(r)$), as pointed out by Bader,[52] is an accurate mapping of the chemical concepts of atom, bond, and structure. The principal topological properties are summarized in terms of their critical points (CP).[52,70] The nuclear positions behave topologically as local maxima in $\rho(r)$. A bond critical point (BCP) is found between each pair of nuclei, which are considered to be linked by a chemical bond, with two negative curvatures, (λ_1 and λ_2) and one positive (λ_3)

(58) Dobado, J. A.; Molina, J. *J. Phys. Chem.* **1994**, *98*, 1819.
(59) Dobado, J. A.; Molina, J. *J. Phys.Chem. A* **1998**, *102*, 788.
(60) Navarro, J. A. R.; Romero, M. A.; Salas, J. M.; Quiros, M.; El-Bahraoui, J.; Molina, J. *Inorg. Chem.* **1996**, *35*, 7829.
(61) El-Bahraoui, J.; Molina, J. *Inorg. Chem.* **1996**, *35*, 7829.
(62) El-Bahraoui, J.; Molina, J.; Portal, D. *J. Phys. Chem. A* **1998**, *102*, 2443.
(63) Cioslowski, J.; Surján, P. R. *J. Mol. Struct. THEOCHEM* **1992**, *255*, 9.
(64) Dobado, J. A.; Martínez-García, H.; Molina, J.; Sundberg, M. R. *Progress in Theoretical Chemistry*; Hernández-Laguna, A., McWeeny, R., Maruany, J., Smeyers, Y. G., Wilson, S., Eds.; Kluwer Academic Publishers: Dordrecht, 1998; in press.
(65) Lee, C.; Yang, W.; Parr, R. G. *Phys. Rev. B* **1988**, *37*, 785.
(66) Becke, A. D. *J. Chem. Phys.* **1993**, *98*, 5648.
(67) Møller, C.; Plesset, M. S. *Phys. Rev.* **1934**, *46*, 618.
(68) Frisch, M. J.; Trucks, G. W.; Schlegel, H. B.; Gill, P. M. W.; Johnson, B. G.; Robb, M. A.; Cheeseman, J. R.; Keith, T.; Petersson, G. A.; Montgomery, J. A.; Raghavachari, K.; Al-Laham, M. A.; Zakrzewski, V. G.; Ortiz, J. V.; Foresman, J.; Cioslowski, B. B.; Stefanov, A.; Nanayakkara, M.; Challacombe, J. B.; Peng, C. Y.; Ayala, P. Y.; Chen, W.; Wong, M. W.; Andres, J. L.; Replogle, E. S.; Gomperts, R.; Martin, R. L.; Fox, D. J.; Binkley, J. S.; Defrees, D. J.; Baker, J.; Stewart, J. J. P.; Head-Gordon, M.; Gonzalez, C.; Pople, J. A. *Gaussian 94*, revision C.2; Gaussian, Inc.: Pittsburgh, PA, 1995.
(69) Biegler-Köning, F. W.; Bader, R. F. W.; Tang, T. H. *J. Comput. Chem.* **1982**, *3*, 317.
(70) For a general review of the AIM theory see: (a) Ref 52. (b) Bader, R. F. W. *Chem. Rev.* **1991**, *91*, 893. (c) Bader, R. F. W. In *Encyclopedia of Computational Chemistry*; Schleyer, P. v. R., Ed.; Wiley & Sons: Chichester, 1998.
(71) Popelier, P. L. A. *Comput. Phys. Commun.* **1996**, *93*, 212.

(denoted as (3,−1) CP). The ellipticity (ϵ) of a bond is defined by means of the two negative curvatures in a BCP as:

$$\epsilon = \lambda_1/\lambda_2 - 1, \qquad where\ |\lambda_2| < |\lambda_1| \tag{1}$$

The ring CPs are characterized by a single negative curvature. Each (3,−1) CP generates a pair of gradient paths[52] which originate at a CP and terminate at neighboring attractors. This gradient path defines a line through the charge distribution linking the neighboring nuclei. Along this line, $\rho(r)$ is a maximum with respect to any neighboring line. Such a line is referred to as an atomic interaction line.[52,70] The presence of an atomic interaction line in such equilibrium geometry satisfies both the necessary and sufficient conditions that the atoms be bonded together.

The Laplacian of the electronic charge density ($\nabla^2\rho(r)$) describes two extreme situations. In the first $\rho(r)$ is locally concentrated ($\nabla^2\rho(r) < 0$) and in the second it is locally depleted ($\nabla^2\rho(r) > 0$). Thus, a value of $\nabla^2\rho(r) < 0$ at a BCP is unambiguously related to a covalent bond, showing that a sharing of charge has taken place. While in a closed-shell interaction, a value of $\nabla^2\rho(r) > 0$ is expected, as found in noble gas repulsive states, ionic bonds, hydrogen bonds, and van der Waals molecules.

Bader has also defined a local electronic energy density ($E_d(r)$), as a functional of the first-order density matrix:

$$E_d(r) = G(r) + V(r) \tag{2}$$

where the $G(r)$ and $V(r)$ correspond to a local kinetic and potential energy density, respectively.[52] The sign of the $E_d(r)$ determines whether accumulation of charge at a given point r is stabilizing ($E_d(r) < 0$) or destabilizing ($E_d(r) > 0$). Thus, a value of $E_d(r) < 0$ at a BCP presents a significant covalent contribution and, therefore, a lowering of the potential energy associated with the concentration of charge between the nuclei. Very recently, for some saturated and unsaturated hydrocarbons, Grimme[72] has found a linear correlation between the bond energies, the $E_d(r)$ and $\rho(r)$ at the position of the BCPs.[74]

III. Results and Discussion

A. Geometrical Description. Calculations on structures **1**−**45** (see Figure 1) have been performed at the theoretical levels described in the methodology. The numerical results are presented inTables 2−4. Table 2 presents the geometrical bond length parameters for the calculated structures, including the non-hypervalent ones for **19**−**27** for comparison. The corresponding valence angle values are given in Table SI. Table 3 shows the numerical parameters at the different bond critical points (BCPs) for X−Z bonds, and the corresponding values for the X−Y bonds are listed in Table SII. In Table 4, the atomic charges calculated by integration over the different basin atoms are shown. Table SIII lists the total energies and the calculated and experimental dipole moments. Table SIV gives the parameters of the maxima in $\nabla^2\rho(r)$. Tables SI to SIV are available as Supporting Information.

Theoretical calculations for several structures depicted in Figure 1 are available in the literature and a summary of the geometrical parameters is presented in Table 1. In general, the theoretical description, available in the literature, and the new structures presented in this work agree with the experimental data. The main differences appear between the theoretical and the experimental S−F or Se−F bond lengths (structures **8**, **14**, and **35**), for which the deviation is ca. 0.07 Å. As mentioned in the Introduction, the S−O bond is described as a highly polarized double bond.[18,51] This statement was partially supported considering the S−O bond length. The S−O distance is markedly shorter in the sulfoxide and sulfones than the standard S−O single bond[75] (1.56 Å) or 1.574 Å for a S−O single bond in sulfuric acid.[76] Higher values have been calculated by Steudel[77] for isomeric forms of H_2S_2O (ca. 1.68 Å). The S−O distances for structures **7** and **9** are ca. 151 and ca. 1.46 Å for **34** and **36** (see Table 2), with >SO or $>SO_2$ fragments, respectively (see Figure 1).

The hypervalent structures (**10** and **12**) containing the S−S bond with the >SS fragment, and **37** and **39** with the $>SS_2$ fragment, have bond distances closer to the standard S−S single bond than to the corresponding S−O counterpart (ca. 2.03 Å for **10** and **12**, and 1.98 Å for **37** and **39** compared to 2.0−2.15

Table 2. Geometrical Bond Length Parameters (Å at the Different Theoretical Levels)

	Z−X			X−Y		
	DFT	MP2	exptl.	DFT	MP2	exptl.
1	1.549	1.493		0.969	0.967	
2	1.160	1.148[a]		1.671	1.683[a]	
3	1.491	1.451		1.447	1.445	
4	1.949	1.921		0.966	0.963	
5	1.503	1.485[a]		1.769	1.798[a]	
6	1.893	1.859		1.449	1.446	
7	1.507	1.502		1.394	1.379	
8	1.437	1.433	1.420[b]	1.652	1.641	1.583[b]
9	1.514	1.508	1.485[c]	1.805	1.806	1.799[c]
10	2.033	2.017		1.375	1.358	
11	1.881	1.853	1.856[d]	1.683	1.677	1.608[d]
12	2.034	2.002		1.858	1.801	
13	1.667	1.657		1.526	1.515	
14	1.593	1.585	1.576[e]	1.801	1.797	1.730[e]
15	1.672	1.663		1.983	1.948	
16	2.140	2.124		1.513	1.499	
17	2.015	1.988		1.827	1.824	
18	2.141	2.117		1.983	1.946	
19				0.964	0.959	0.958
20				1.407	1.405	1.405
21				1.411	1.409	1.410
22				1.350	1.341	1.336
23				1.639	1.628	1.589
24				1.824	1.802	1.802
25				1.480	1.474	1.460‘
26				1.786	1.778	
27				1.970	1.948	1.945[f]
28	1.525	1.468		0.976	0.979	
29	1.236			1.745		
30	1.489	1.441		1.500	1.497	
31	2.033	2.002		0.972	0.971	
32	1.599	1.604[a]		1.958	1.898[a]	
33	1.993	1.944		1.497	1.489	
34	1.456	1.449		1.373	1.363	
35	1.426	1.420	1.405[g]	1.596	1.583	1.530[g]
36	1.466	1.459	1.431[c]	1.808	1.782	1.777[c]
37	1.973	1.942		1.375	1.363	
38	1.895	1.868		1.656	1.641	
39	1.985	1.952		1.831	1.795	
40	1.627	1.613		1.511	1.503	
41	1.595	1.581		1.759	1.746	
42	1.636	1.622		1.957	1.918	
43	2.100	2.068		1.511	1.501	
44	2.034	2.001		1.807	1.794	
45	2.111	2.077		1.974	1.931	

[a] At the CCD/6-311G*//CCD/6-311+G* theoretical level. [b] Reference 90. [c] Reference 87. [d] Reference 91. [e] Reference 92. [f] Reference 89. [g] Reference 93.

(72) Grimme, S. *J. Am. Chem. Soc.* **1996**, *118*, 1529.

(73) Koput, J. *J. Mol. Spectrosc.* **1986**, *115*, 438.

(74) $E_d(r)$ values (hartree/bohr^3) for several covalent and ionic molecules are the following: H_2, −0.262; N_2, −1.54; CH_4, −0.262; HF, −0.588; HLi, 0.0012.

(75) Kucsman, A.; Kapovits, I. *Organic Sulphur Chemistry*; Bernardi, F., Csizmadia, I. G., Magnini, A., Eds.; Elsevier: Amsterdam, 1985; Chapter 3.

(76) Cotton, F. A.; Wilkinson, G. *Advanced Inorganic Chemistry*, 5th ed.; Wiley-Interscience: New York, 1988.

Table 3. The Electron Charge Density, $\rho(r)$, Its Laplacian, $\nabla^2\rho(r)$, Ellipticity, ϵ, Electronic Energy Density, $E_d(r)$, and λ_1/λ_3, at the Different Theoretical Levels of Structures **1**−**18** and **28**−**45**, for the X−Z BCPs

	$\rho(r)$ (e/a_o^3)		$\nabla^2\rho(r)$ (e/a_o^5)		ϵ		$E_d(r)$		λ_1/λ_3	
	DFT	MP2	DFT	MP2	DFT	MP2	DFT	MP2	DFT	MP2
1	0.191	0.226	0.365	0.310	0.020	0.019	−0.085	−0.134	0.336	0.376
2	0.612	0.636[a]	−1.005	−1.202[a]	0.010	0.003[a]	−0.850	−0.955[a]	0.715	0.761[a]
3	0.232	0.262	0.290	0.223	0.024	0.022	−0.131	−0.179	0.388	0.422
4	0.089	0.091	0.130	0.132	0.020	0.012	−0.034	−0.042	0.278	0.261
5	0.242	0.251[a]	1.033	1.248[a]	0.040	0.034[a]	−0.251	−0.261[a]	0.198	0.187[a]
6	0.105	0.110	0.095	0.087	0.030	0.018	−0.052	−0.066	0.342	0.343
7	0.265	0.262	0.425	0.566	0.012	0.012	−0.325	−0.318	0.324	0.289
8	0.299	0.295	1.222	1.366	0.009	0.002	−0.353	−0.343	0.226	0.211
9	0.263	0.260	0.415	0.554	0.033	0.031	−0.322	−0.315	0.330	0.294
10	0.138	0.141	−0.060	−0.074	0.026	0.028	−0.079	−0.088	0.645	0.695
11	0.196	0.205	−0.255	−0.300	0.032	0.029	−0.164	−0.188	1.294	1.730
12	0.145	0.150	−0.085	−0.107	0.010	0.014	−0.084	−0.096	0.694	0.766
13	0.210	0.221	0.219	0.163	0.004	0.003	−0.163	−0.187	0.369	0.402
14	0.249	0.258	0.503	0.500	0.008	0.015	−0.216	−0.237	0.307	0.318
15	0.209	0.209	0.221	0.289	0.002	0.001	−0.162	−0.167	0.368	0.341
16	0.124	0.126	−0.027	−0.034	0.020	0.022	−0.060	−0.065	0.572	0.597
17	0.160	0.166	−0.077	−0.081	0.027	0.033	−0.098	−0.108	0.670	0.679
18	0.127	0.131	−0.038	−0.049	0.008	0.011	−0.061	−0.069	0.594	0.628
28	0.202	0.239	0.421	0.358	0.022	0.011	−0.098	−0.154	0.328	0.366
29	0.477		−0.290		0.031		−0.552		0.579	
30	0.231	0.266	0.357	0.282	0.016	0.007	−0.131	−0.187	0.366	0.401
31	0.074	0.075	0.157	0.161	0.005	0.006	−0.018	−0.024	0.230	0.332
32	0.183	0.178[b]	0.519	0.565[a]	0.008	0.044[a]	−0.174	−0.170[a]	0.205	0.190[a]
33	0.083	0.090	0.141	0.136	0.029	0.019	−0.026	−0.038	0.262	0.262
34	0.292	0.290	0.951	1.122	0.038	0.028	−0.353	−0.346	0.257	0.237
35	0.311	0.309	1.202	1.365	0.047	0.044	−0.380	−0.374	0.236	0.220
36	0.288	0.286	0.852	1.015	0.034	0.028	−0.350	−0.344	0.268	0.246
37	0.158	0.166	−0.116	−0.154	0.000	0.002	−0.107	−0.129	0.781	0.959
38	0.182	0.190	−0.195	−0.205	0.009	0.004	−0.162	−0.195	1.245	1.643
39	0.157	0.165	−0.117	−0.152	0.005	0.002	−0.103	−0.124	0.780	0.927
40	0.231	0.234	0.294	0.405	0.014	0.010	−0.194	−0.203	0.356	0.323
41	0.247	0.251	0.355	0.486	0.020	0.019	−0.218	−0.227	0.345	0.312
42	0.228	0.231	0.278	0.376	0.010	0.008	−0.189	−0.198	0.359	0.329
43	0.133	0.140	−0.038	−0.056	0.019	0.022	−0.070	−0.081	0.596	0.650
44	0.148	0.156	−0.061	−0.077	0.035	0.037	−0.089	−0.101	0.657	0.704
45	0.132	0.139	−0.418	−0.059	0.007	0.012	−0.069	−0.079	0.602	0.652

[a] At the CCD/6-311+G*//CCD/6-311+G* theoretical level.

Å for standard disulfide distances,[76] and also in the same range as the values reported by Steude.[77]

Additional shortening of the S−Z (Z = O, S) bond lengths was observed passing from >SZ to <SZ_2 fragments for all of the above mentioned structures. This behavior is also present in the >SeZ fragment (**13**, **15**, **16**, and **18**) compared to >SeZ_2 (**40**, **42**, **43** and **45**) with Z = O, S (see Table 2).

Further shortening in the X−Z bond distances was found when the Y group (see Figure 1) was fluorine instead of hydrogen or methyl. This shortening provided smaller (ca. 0.03−0.07 Å) values for the Z = O moieties than for the Z = S analogs (ca. 0.08−0.15 Å, see Table 2).

The geometrical characteristics for the structures considered are markedly different when the central atom X is oxygen. The X−Z bond lengths were longer than the standard X−Z single bonds (ca. 1.5 Å) for X = O (**1**, **3**, **28**, and **30**) vs 1.464 Å for hydrogen peroxide,[73] and ca. 2.0 Å for X = S (**4**, **6**, **31**, and **33**) vs 1.574 Å for the S−O single bond in sulfuric acid.[76]

The O−Z bond shortening (ca. 0.4 Å) was more remarkable than that in the S−Z and Se−Z bonds for structures with fluorine atoms (**2**, **5**, **29**, and **32**) compared to structures with hydrogen and methyl groups. This shortening was observed together with a considerable lengthening in the O−F bond (>0.26 Å). The value for **2** (1.671 Å) was higher than the standard single O−F bond in **20** (1.407 Å) (see Table 2). The overall description is in good agreement with the experimental data when available at both B3LYP and MP2 levels (see Table 2). However, from Table 2, systematic trends are evident between the two levels. The overall DFT bond lengths are greater than the corresponding MP2 ones from Z−X and Y−X. The average difference is 0.024 Å for the X−Z bond average and 0.013 Å for X−Y bonds. The root mean square is 0.015 and 0.016, respectively. In addition, the MP2 values are consistent in better agreement with the experimetal results.

B. Bond Nature in Y_2OZ and Y_2OZ_2 Structures. This section discusses the structures with highly electronegative oxygen as a central atom (**1**−**6** and **28**−**33**; Figure 1) in more detail, owing to the special geometrical characteristics described in the previous section (very long O−Z bond lengths). Obviously, the eletronic properties of the central atom must differ considerably from those of the other chalcogens, leading to different bonding characteristics.

Figure 2 depicts $\nabla^2\rho(r)$ contour maps for structures **1**, **2**, **4**, and **5**. Structure **1** shows a small interaction between the two oxygen atoms. The electron charge concentration surrounds the H_2O substructure with a large area of positive $\nabla^2\rho(r)$ values (charge depletion) in the O−O bond region. Also the charge concentration corresponding to the electron pair responsible for the coordinate bond appears clearly in the surroundings of the central oxygen atom. This representation is largely the same for structures **3**, **4**, **6**, **28**, **30**, **31**, and **33**. The above description is compatible with the numerical properties obtained at the BCPs

(77) Steudel, R.; Drozdova, Y.; Hertwig, R. H.; Koch, W. *J. Phys. Chem.* **1995**, *99*, 5319.

Table 4. Bader's Atomic Charges for Structures **1**−**18** and **28**−**45**

	DFT	MP2		DFT	MP2		DFT	MP2
1@*O*[a]	−0.72	−0.73	**2**@*O*[a]	0.39	0.37[b]	**3**@*O*[a]	−0.68	−0.66
@*O*	−0.47	−0.51	@*O*	0.11	0.09[b]	@*O*	−0.51	−0.55
@*H*	0.59	0.61	@*F*	−0.25	−0.23[b]	@*C*	0.34	0.30
4@*O*[a]	−0.97	−1.03	**5**@*O*[a]	−0.42	−0.59[b]	**6**@*O*[a]	−0.93	−0.96
@*S*	−0.22	−0.21	@*S*	1.03	1.10[b]	@*S*	−0.23	−0.22
@*H*	0.60	0.62	@*F*	−0.30	−0.26[b]	@*C*	0.34	0.30
7@*S*[a]	1.15	1.18	**8**@*S*[a]	2.26	2.33	**9**@*S*[a]	1.19	1.27
@*O*	−1.17	−1.21	@*O*	−1.15	−1.16	@*O*	−1.20	−1.24
@*H*	0.01	0.01	@*F*	−0.55	−0.58	@*C*	−0.20	−0.28
10@*S*[a]	0.21	0.21	**11**@*S*[a]	1.07	1.09	**12**@*S*[a]	0.25	0.32
@*S*	−0.34	−0.37	@*S*	−0.02	0.02	@*S*	−0.40	−0.41
@*H*	0.06	0.06	@*F*	−0.53	−0.56	@*C*	−0.17	−0.25
13@*Se*[a]	1.11	1.29	**14**@*Se*[a]	1.97	2.32	**15**@*Se*[a]	1.14	1.24
@*O*	−0.93	−1.07	@*O*	−0.86	−1.04	@*O*	−0.98	−1.01
@*H*	−0.09	−0.11	@*F*	−0.55	−0.64	@*C*	−0.29	−0.38
16@*Se*[a]	0.54	0.52	**17**@*Se*[a]	1.33	1.37	**18**@*Se*[a]	0.59	0.66
@*S*	−0.43	−0.45	@*S*	−0.24	−0.23	@*S*	−0.50	−0.52
@*H*	−0.05	−0.04	@*F*	−0.55	−0.57	@*C*	−0.27	−0.36
28@*O*[a]	−0.53	−0.48	**29**@*O*[a]	0.38		**30**@*O*[a]	−0.39	−0.33
@*O*	−0.39	−0.43	@*O*	0.04		@*O*	−0.44	−0.48
@*H*	0.66	0.67	@*F*	−0.23		@*C*	0.27	0.21
31@*O*[a]	−0.97	−1.02	**32**@*O*[a]	−0.74	−0.77[b]	**33**@*O*[a]	−0.85	−0.88
@*S*	−0.16	−0.14	@*S*	0.77	0.68[b]	@*S*	−0.17	−0.17
@*H*	0.64	0.66	@*F*	−0.41	−0.30[b]	@*C*	0.26	0.22
34@*S*[a]	2.37	2.44	**35**@*S*[a]	3.50	3.64	**36**@*S*[a]	2.36	2.49
@*O*	−1.23	−1.26	@*O*	−1.18	−1.22	@*O*	−1.26	−1.29
@*H*	0.05	0.04	@*F*	−0.57	−0.61	@*C*	−0.19	−0.28
37@*S*[a]	0.28	0.28	**38**@*S*[a]	0.97	0.97	**39**@*S*[a]	0.33	0.39
@*S*	−0.23	−0.24	@*S*	0.04	0.08	@*S*	−0.29	−0.29
@*H*	0.09	0.10	@*F*	−0.53	−0.56	@*C*	−0.16	−0.25
40@*Se*[a]	1.91	2.00	**41**@*Se*[a]	2.62	2.74	**42**@*Se*[a]	1.92	2.09
@*O*	−0.92	−0.96	@*O*	−0.80	−0.83	@*O*	−0.96	−1.00
@*H*	−0.04	−0.04	@*F*	−0.51	−0.53	@*C*	−0.28	−0.39
43@*Se*[a]	0.73	0.77	**44**@*Se*[a]	1.33	1.40	**45**@*Se*[a]	0.77	0.89
@*S*	−0.34	−0.37	@*S*	−0.14	−0.15	@*S*	−0.41	−0.43
@*H*	−0.02	−0.02	@*F*	−0.53	−0.55	@*C*	−0.26	−0.36

[a] Central atom. [b] At the CCD/6-311+G*//CCD/6-311+G* theoretical level.

in the O−O or O−S bonds (see Table 3). The electron density is relatively low (ca. 0.1 and 0.2 e/a_o^3) for the O−S and O−O BCPs, respectively. The $\nabla^2\rho(r)$ values are positive and also of the same order of magnitude. On the other hand, the $E_d(r)$ values are negative but small, indicating a weak closed-shell interaction, compatible with λ_1/λ_3 values (between ca. 0.2 and 0.3, see Table 3).

The observations discussed above agree with a coordinate bond where a small amount of electron density is donated by the central oxygen atom. This representation changes dramatically if the hydrogen atoms or the methyl groups connected to the central oxygen atom are replaced by fluorine (**2**, **5**, **29**, and **32**). The bond distances decrease ca. 0.4 Å from the parent compounds (**1**, **4**, **28**, and **31**) with hydrogen (see Table 2). Figure 2 illustrates considerable increase in electron charge concentration in the O−Z bond region for structures **2** and **5**. Also, structures **29** and **32** yielded similar $\nabla^2\rho(r)$ contour plots (available as Supporting Information, Figure S1). It is noteworthy that the shortening of the O−Z bond and increased charge density of the bond also resulted in concomitant increase in delocalization of the electron pairs of the acceptor atom. This delocalization can be observed from the $-\nabla^2\rho(r)$ numerical values of the acceptor atom; these values decrease when fluorine atoms replace the hydrogen or methyl groups (see Table SII). Structures **2** and **29**, in which Z = O, have strong covalent bonds. This is seen in the $\rho(r)$ values of ca. 0.6 and 0.5 e/a_o^3, respectively. Further corroboration comes from the high and negative $\nabla^2\rho(r)$ values of ca. −1.0 and −0.3 e/a_o^5, respectively. Moreover, the $E_d(r)$ values become high and negative (−0.85 and −0.55 hartree/au, respectively). The λ_1/λ_3 values are also compatible with a covalent bond (see Table 3).

The same trend was also observed when Z = S (structures **5** and **32**). Although in this particular case the $\rho(r)$ values are larger than the corresponding ones for the parent compounds (**4** and **31**), the $\nabla^2\rho(r)$ is high and positive (ca. 1.0 and 0.5 e/a_o^5 for **5** and **32**, respectively). The $E_d(r)$ values remain negative and higher than the corresponding values for **4** and **31**. These numerical values resemble the situation in the C−O and C−S multiple bonds.[78]

On the other hand, increased F−O bond elongation is detected for **2**, **5**, **29**, and **32**, compared to the F−O bond in **20** (see Table 2). The F−O bond in these structures shows characteristics of a decidedly ionic and unstable bond (low $\rho(r)$ and λ_1/λ_3 values, positive $\nabla^2\rho(r)$ values, and very low $E_d(r)$ values, see Table SII). Furthermore, a positive $\nabla^2\rho(r)$ region was observed in Figure 2 in the F−O bond region of structures **2** and **5**, as in structures **29** and **32**, too (see Figure S1 in Supporting Information).

In addition, the Z atoms lose a large amount of negative charge (see Table 4) when the two fluorine atoms are present. For example, passing from **1** to **2** the Z atomic charge varies from −0.47 to 0.11, respectively, from **4** to **5** the corresponding charges change form −0.22 to 1.03, etc.

These results are compatible with the following bond description: structures without fluorine **1**, **3**, **4**, **6**, **28**, **30**, **31**, and **33** show a very weak coordinate σ-bond with a small amount of electron density donated from the central oxygen to the Z atoms,

(78) See ref 52, p 311.

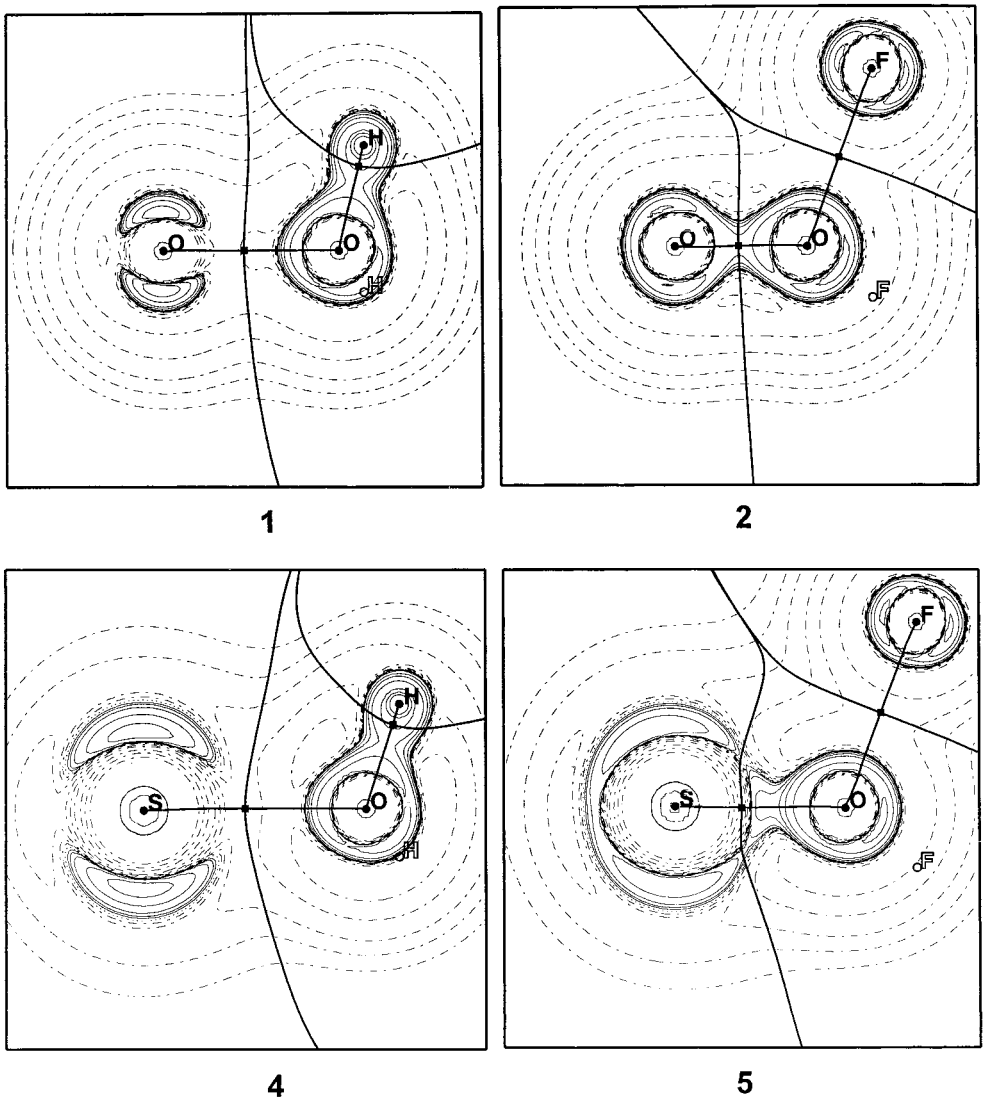

Figure 2. $\nabla^2\rho(r)$ contour maps, in the molecular plane obtained with use of the MORPHY program,[71] for structures **1**, **2**, **4**, and **5** calculated at the B3LYP/6-311+G* level. The contours begin at zero and increase (solid contours) and decrease (dashed contours) in steps of ±0.02, ±0.04, ±0.08, ±0.2, ±0.4, ±0.8, ±2.0, ±4.0, and ±8.0. The thick solid lines represent the molecular graph that joins the nuclei (solid circles) and the BCP (solid squares) and the BCP (solid squares), and also the zero flux surface.

giving bond lengths longer than for the corresponding O−Z single bonds and small atomic charges on Z atoms. However, an O−Z bond shortening and an F−O bond lengthening is observed, together with a large amount of electron charge concentration in the O−Z bond region, when fluorine atoms are present (**2**, **5**, **29**, and **32**). These facts strongly suggest the presence of negative hyperconjugation, i.e., π donation from the Z atom to the O−F σ* bond. This is also in accordance with the loss of electron charge concentration in the Z atom surroundings for fluorinated structures, where $\nabla^2\rho(r)$ values change from −6.41 to −4.75 e/a_o^5 when compared with the parent compounds (see Table SII). From all these considerations, we conclude that structures **1**, **3**, **4**, **6**, **28**, **30**, **31**, and **33** cannot be deemed hypervalent molecules, although structures **2**, **5**, **29**, and **32** are hypervalent.

C. Bond Nature in Y_2XZ and Y_2XZ_2 (X = S, Se; Z = O, S) Structures. The electronic properties of the X−Z bonds are entirely different from those of the O−Z bonds discussed in the previous subsection B. Now, the central atom is S or Se and the coordinate bonds have large electron density donated by the central atom to the corresponding acceptor atoms. This is clearly depicted in Figure 3, in which the main electron charge concentration of the X−Z bond region belongs to the Z atoms. However, for structures **10** and **11** (where X and Z are equal to S) the electron charge concentration is shared by both sulfur atoms. On the other hand, structures **34**−**45** (with two Z atoms) together with **9**, **12**, **15**, and **18** have a $\nabla\ ^2\rho(r)$ topological description qualitatively similar to that of the structures depicted in Figure 3. The $\nabla^2\rho(r)$ contour maps for these structures are also available as Supporting Information as Figure S2.

Numerically, the X−O bonds are compatible with our previous P−O bond description for hypervalent molecules.[1] The electronic charge densities have medium values, the $\nabla^2\rho(r)$ with high and positive and the $E_d(r)$ negative values, all of them being typical for a polarized σ-bond. The atomic charges on oxygen are ca. −1.0.

Cioslowski *et al.*[63] proposed a similar description but with the participation of an ionic π-bond for compounds containing >SO and $>SO_2$ fragments. In this ionic π-bond more than 90% of the charge density belongs to the oxygen atoms. However, this participation can also be represented as an unshared electron pair on oxygen. The non-involvement of the π-bond is also compatible with the X−H or X−C bond lengths found in structures **7**, **9**, **13**, **15**, **36**, **40**, and **42** compared to structures

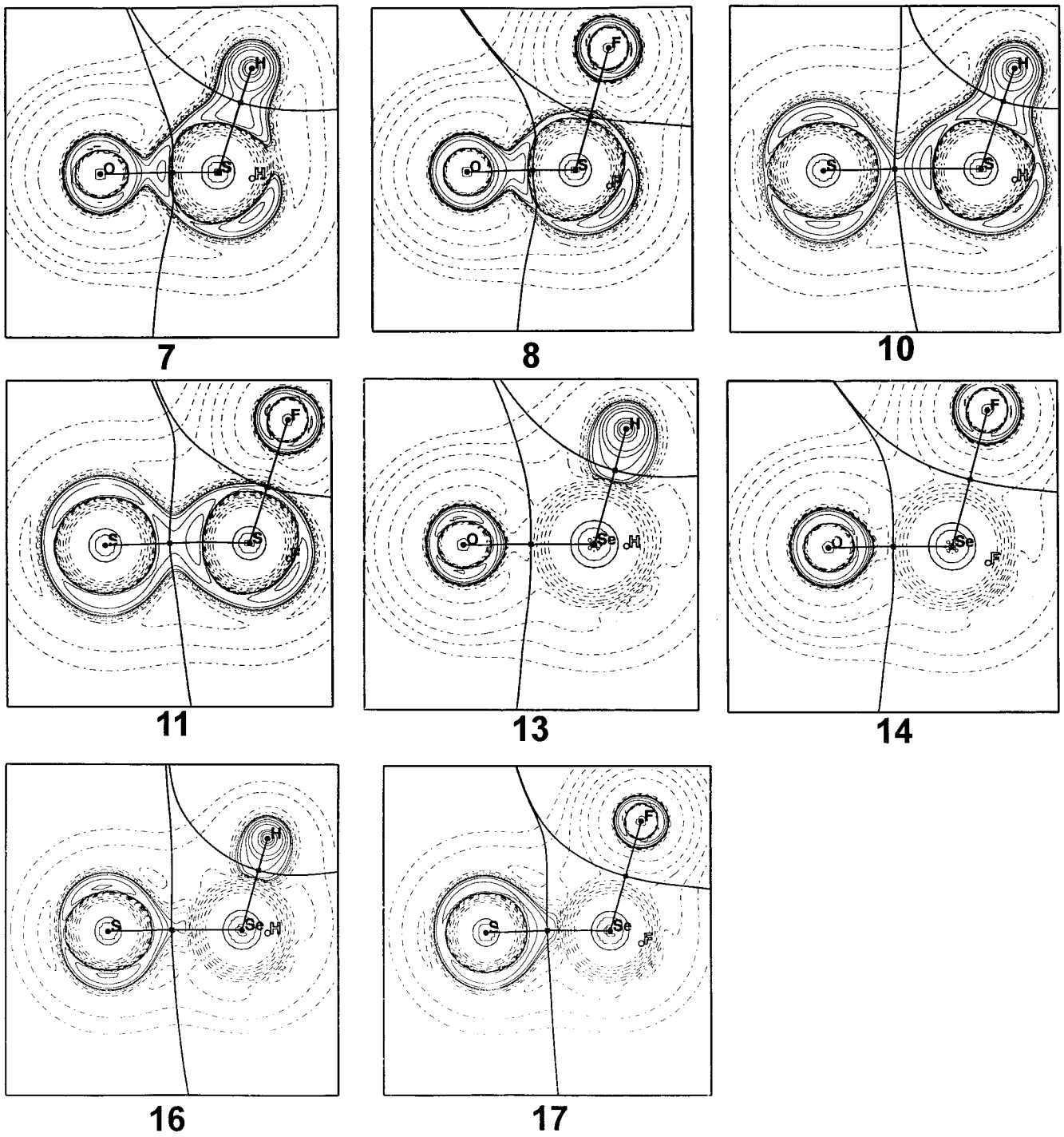

Figure 3. $\nabla^2\rho(r)$ contour maps, in the molecular plane obtained with use of the MORPHY program,[71] for structures **7**, **8**, **10**, **11**, **13**, **14**, **16**, and **17** calculated at the B3LYP/6-311+G* level. The contours begin at zero and increase (solid contours) and decrease (dashed contours) in steps of ±0.02, ±0.04, ±0.08, ±0.2, ±0.4, ±0.8, ±2.0, ±4.0, and ±8.0. The thick solid lines represent the molecular graph that joins the nuclei (solid circles) and the BCP (solid squares), and also the zero flux surface.

22, **24**, **25**, and **29** (see Table 2). The π-back-bonding participation has been invoked to explain the shortening in the X−O bond for fluorinated structures.[79] However, in our case it is not necessary to introduce this π-back-bonding contribution for **8**, **14**, **35**, and **41**. In fact, an X−O bond shortening takes place for these structures compared to the parent ones (see Table 2). However, the lengthening in the X−F bond is small, or even negligible. In addition, the atomic charges on oxygen remain mainly unchanged in comparison with, e.g., structures **7** and **8** (−1.17 and −1.15, respectively, see Table 4). In the same way, the numerical BCP properties remain almost invariant. Thus, this shortening could be produced mainly by electrostatic interactions (the atomic charges on oxygen remain unchanged and negative, but on X atoms they increase to higher positive values).

(79) Yang, C.; Goldstein, E.; Breffle, S.; Jin, S. *J. Mol. Struct. THEOCHEM* **1992**, *259*, 345.

(80) Fueno, H.; Ikuta, S.; Matsuyama, H.; Kamigata, N. *J. Chem. Soc., Perkin Trans. 2* **1992**, 1925.

(81) Francl, M. M.; Pietro, J.; Hehre, W. J.; Binkley, J. S.; Gordon, M. S.; DeFrees, D. J.; Pople, J. A. *J. Chem. Phys.* **1982**, *77*, 3654.

(82) Speers, P.; Laidig, K. E.; Streitwieser, A. *J. Am. Chem. Soc.* **1994**, *116*, 9257.

When Z = S (structures **10**−**12**, **16**−**18**, **36**−**39**, and **43**−**45**) the electronegativity difference between the X and Z atoms becomes extremely small or even zero, comparable to the compounds discussed in subsection B. However, the situation now is different. There is an electron charge concentration in the X−Z bond region (see Figure 3). Numerically, the S−S bond length is similar to the S−S single bond in HSSH structure, calculated at the same theoretical level (2.033 and 2.110 Å, respectively). The numerical properties of the S−S BCPs in **10** and **12** correspond to weak covalent bond (small $\rho(r)$ values of ca. 0.13 e/a_o^3, and small and negative $\nabla^2\rho(r)$ and $E_d(r)$ values of ca −0.06 e/a_o^5 and −0.08 hartree/au, respectively). The λ_1/λ_3 values (0.6) agree with a covalent bond, however. The atomic charges are small on the terminal sulfur atoms (−0.4).

Upon changing hydrogen to fluorine in structure **11**, a moderate shortening is observed for the S−S bond. However, no elongation appears in the S−F bond. The S−S bond region in **11** shows marked covalency with higher values for $\rho(r)$, and higher and negative values for $\nabla^2\rho(r)$, ca. 0.2 e/a_o^3 and −0.25 e/a_o^5, respectively. In this case, the $E_d(r)$ gives higher negative values showing stabilization for the S−S bond. The atomic charge on the terminal sulfur atom decreases moderately to give a very small value (−0.02). However, this value increases to a higher and positive one (ca. 1.1) for the central sulfur atom.

All these faccts characterize the differences of structure **11** from **2** to **5**. Now, the bond shortening and stabilization is explained only by the electronic charge concentration in the bond region, due to electrostatic interactions with the highly positive charges on the sulfur central atom, when two fluorine atoms are presented.

For X = Se, the main electronic interactions are completely similar to those previously presented for structures **11** and **12**. They support the concept of a weak Se−S bond with similar numerical values at the BCPs. The strength of this bond increases also for the fluorinated structures.

IV. Conclusions

Calculations on oxygen, sulfur, and selenium hypervalent structures have been performed comparing B3LYP and MP2 results. The geometrical values agree with the experimental data when available. However, the MP2 results are the closest to the experimental data. When the central atoms is oxygen, a weak coordinate bond is observed with a small amount of $\rho(r)$ involved in the bond. The strength of this bond increases spectacularly when two fluorine atoms are bonded to the central oxygen atom. This is due mainly to negative hyperconjugative π-back-donation form the Z atom to the O−F σ^*-bond (yielding very long O−F bond lengths).

The bond nature in the hypervalent structures with X = S or Se as central atoms is characterized as a polarized single σ-bond with its strength depending mainly on electrostatic interactions. The central and terminal atoms carry positive and negative charges, respectively, and consequently cannot be considered to be hypervalent molecules.

The description for X−Z (X = S, Se; Z = O, S) has remarkable resemblance with our previous result for pnicogen (N, P, As)−chalcogen(O, S) bonds.

Acknowledgment. Computing time was provided by the Universidad de Granada (Spain). We are grateful to Professor R. W. F. Bader for a copy of the AIMPAC package of programs and to Professor P. L. A. Popelier for a copy of the MORPHY program. We thank David Nesbitt for language revision of the original English manuscript.

Supporting Information Available: Table S1, geometrical bond angle parameters at the different theoretical levels; Table SII, the electron charge density, $\rho(r)$, its Laplacian, $\nabla^2\rho(r)$, ellipticity, ϵ, electronic energy density, $E_d(r)$, and λ_1/λ_3, at the different theoretical levels of structures **1**−**18** and **28**−**45**, for the X−Y BCPs; Table SIII, total energies and the calculated and experimental dipole moments for structures **1**−**45**; Table SIV, parameters in the $\nabla^2\rho(r)$ maxima for structures **1**−**18** and **28**−**45**; Figure S1, $\nabla^2\rho(r)$ contour maps for structures **3**, **6**, and **28**−**33**; Figure S2, $\nabla^2\rho(r)$ contour maps for structures **9**, **12**, **15**, **18**, and **34**−**45** (PDF). This material is available free of charge via the Internet at http://pubs.acs.org.

JA9828206

(83) Schmiedekamp, A.; Cruickshank, D. W. J.; Skaarup, S.; Pulay, P.; Hargittai, I.; Boggs, J. E. *J. Am. Chem. Soc.* **1979**, *101*, 2002.
(84) Tossell, J. A. *Chem. Phys.* **1991**, *154*, 211.
(85) Koch, R.; Anders, E. *J. Org. Chem.* **1994**, *59*, 4529.
(86) Lide, D. R. *CRC Handbook of Chemistry and Physics*, 78th ed.; CRC Press: Oxford, 1997.
(87) Hehre, W. J.; Radom, L.; Schleyer, P. v. R.; Pople, J. A. *Ab initio Molecular Orbital Theory*; Wiley-Interscience: New York, 1986.
(88) Lide, D. R.; Mann, D. E. *J. Chem. Phys.* **1958**, *29*, 914.
(89) Pairier, R. A.; Csizmadia, I. G. *The Chemistry of Organic Selenium and Tellurium Compounds*; Peter, S., Rappoport, Z., Eds.; Wiley-Interscience: New York, 1986; Vol. 1.
(90) Lide, D. R.; Mann, D. E.; Fristrom, R. M. *J. Chem. Phys.* **1957**, *26*, 734.
(91) Marsden, C. J.; Oberhammer, H.; Lösking, O.; Willner, H. *J. Mol. Struct.* **1989**, *193*, 233.
(92) Bühl, M.; Thiel, W.; Fleischer, U.; Kutzelnigg, W. *J. Phys. Chem.* **1995**, *99*, 4000.
(93) Hargittai, I.; Mijlhoff, F. C. *J. Mol. Struct.* **1973**, *16*, 69.
(94) Johnson, D. R.; Powell, F. X. *Science* **1969**, *164*, 950.
(95) Kuczkowski, R. L. *J. Am. Chem. Soc.* **1964**, *86*, 3617.
(96) Pierce, L.; Jackson, R. H. DiCianni, N. *J. Chem. Phys.* **1961**, *35*, 2240.
(97) McClellan, A. *Table of Experimental Dipole Moments*; Rahara Enterprises: 1973; Vol. 2.